PERGAMON

Energy Conversion & Management 41 (2000) 737–756

ENERGY CONVERSION & MANAGEMENT

www.elsevier.com/locate/enconman

Design and thermal analysis of a two stage solar concentrator for combined heat and thermoelectric power generation

Siddig A. Omer[a,*], David G. Infield[b]

[a]*School of the Built Environment, University of Nottingham, University Park, Nottingham, NG7 2RD, UK*
[b]*Centre for Renewable Energy Technology, Loughborough University, Loughborough, LE11 3TU, UK*

Abstract

A design procedure and thermal performance analysis of a two stage solar energy concentrator suited to combined heat and thermoelectric power generation are presented. The concentrator is comprised of a primary one axis parabolic trough concentrator and a second stage compound parabolic concentrator mounted at the focus of the primary. The thermoelectric device is attached to the absorber plate at the focus of the secondary. A cooling tube is fitted to the cold side of the thermoelectric device to extract the waste heat and maintain a high temperature gradient across the device to improve conversion efficiency. The key requirements of the concentrator design are to be tolerant of tracking misalignment, maintain temperature gradients to suit thermoelectric generation and minimise heat losses. A design methodology is presented which allows interception of rays within an angular region ($\pm\delta$). This results in a wider receiver for the parabolic trough concentrator than would usually be used for a similar concentration ratio. The role of the second stage concentrator in limiting heat losses from the absorber plate is evaluated. Results indicate that in addition to improving the concentration efficiency, the second stage compound parabolic concentrator of the proposed design also inhibits convective air movement and, consequently, improves the overall performance of the solar concentrator.

Keywords: Solar energy; Two stage concentrator; Combined heat and power generation; Thermal analysis; Thermoelectric power generation

* Corresponding author. Tel.: +44-115-951-3177; fax: +44-115-951-3159.
E-mail address: siddig.omer@nottingham.ac.uk (S.A. Omer).

0196-8904/00/$ - see front matter
PII: S0196-8904(99)00134-X

1. Introduction

Application of solar thermoelectric (STE) generation has, to date, been limited due to its present low conversion efficiency and high material cost. As a result, very little research effort has been devoted to the use of thermoelectric devices for solar energy conversion in general and terrestrial solar energy conversion in particular. Most of the recent research activities on applications of thermoelectric power generation have been directed towards utilisation of industrial waste heat [1,2].

Because of their capability of operation at elevated temperatures, thermoelectric devices are attractive for applications with concentrated solar energy. The power per unit of material and, hence, the power per unit cost can be increased significantly in this way. They also offer a distinct advantage when used in a cogeneration system which simultaneously provides electrical power and useful heat (extracted from the cold junction of the thermoelectric device). This combination will improve the overall energy conversion efficiency of the system and increase its cost effectiveness. In the case of small scale applications typical of rural power supply, where limited electricity is needed for lighting and appliances, commercially available Peltier thermoelectric devices can be used. These have been developed principally for Peltier cooling. However, they can also be used for power generation. They operate in the temperature range under 500 K, which can be obtained by concentrating solar radiation by a factor of about 20 [3]. When adjusted to produce adequate alignment, a single line focusing parabolic trough concentrator (PTC) would be sufficient. However, this requires high tracking accuracy [4].

At lower concentrations, an appropriate solar concentrator is the compound parabolic concentrator (CPC). This can come close to the maximum theoretical concentration efficiency [5] and is less dependent on tracking accuracy. However, this has the major drawback that the ratio of the concentrator's depth to the reflector aperture becomes excessive and impractical at the above required concentration ratio.

A promising approach is to design the PTC for a low concentration factor and use it in conjunction with a secondary receiver to collect and further concentrate the radiation onto a smaller absorber plate. This allows an amount of tracking error without a significant associated reduction in performance. Several published papers describe designs based on this concept [4,6–8]. A two stage concentrator using a second stage CPC and a primary Fresnel mirror field as a central receiver has been described by Ref. [4]. More recently, Brunotte et al. [8] have described a two stage arrangement giving concentration ratios up to 300 using a north–south polar axis primary PTC with a row of filled dielectric non-imaging 3D concentrators, designed for photovoltaic conversion. Although the design achieves a high concentration ratio, its tolerance to the incoming rays is very limited. Mills [9,10] described a combination of a primary parabolic trough and intermediate asymmetrical CPC secondary, providing concentration ratios in the range 9–12. The design is suggested for both photovoltaic conversion using optical prisms and thermal processes.

In this paper, we present a design and performance evaluation for a two stage solar concentrator. The design is well suited to commercially available thermoelectric devices for small scale power generation. The concentrator is comprised of a primary one axis PTC and a second stage made of a symmetrical CPC, mounted at the focus of the primary. The design developed here is based on a wider receiver than usual for the primary concentrator, allowing

interception of incoming rays within the angular region ($\pm\delta$) which is defined as the tolerance of the concentrator to the incoming radiation.

2. Design of the two stage concentrator

2.1. Optical design

First, a relation between the geometrical concentration ratio, the half angle subtended by the arc of the parabola (rim angle) and the tolerance angle is formulated for the PTC. The contribution of the second stage concentrator is then determined. Finally, optimal rim and tolerance angles are identified that provide the required concentration ratio, with due consideration to other practical constraints.

The system is configured as shown in Fig. 1 where AA′ is the aperture plane of the primary concentrator. The entrance aperture BB′ of the CPC, shown in the figure, acts as a receiver to the PTC. Efficient concentration requires that BB′ should be sufficiently wide to intercept all the rays reflected from the primary within the angular region $\pm\delta$ from the normal. B and B′

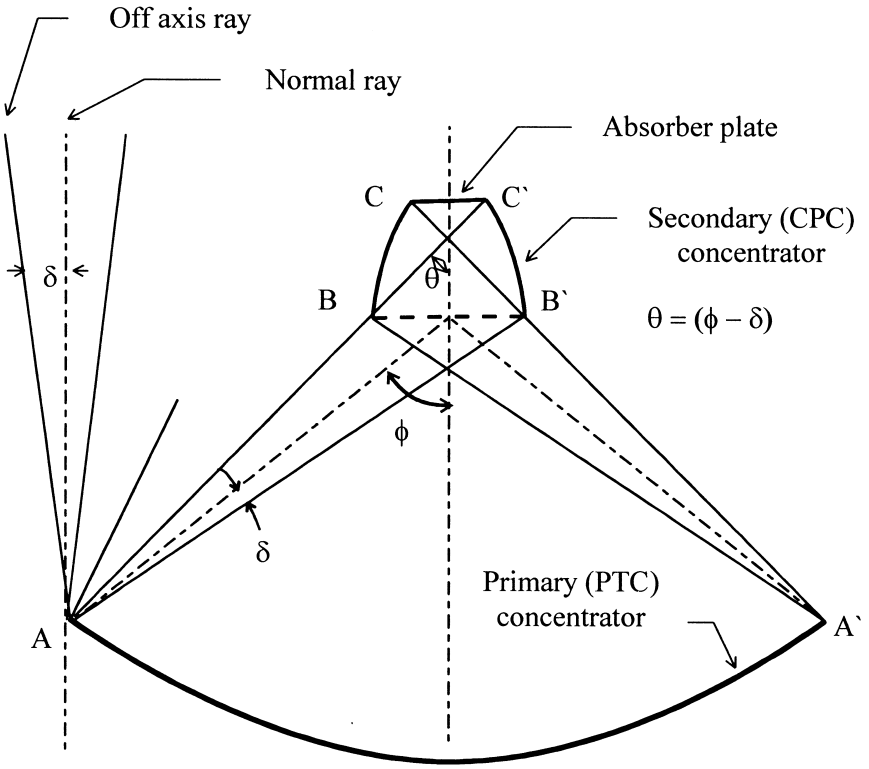

Fig. 1. Two stage concentrator with a primary PTC and a single symmetrical CPC secondary.

are located at the intersections of the extreme rays reflected from A and A′, to C and C′, respectively.

The geometrical concentration ratio of the PTC is given simply by

$$Cr_{(\mathrm{PTC})} = \frac{\mathrm{AA}'}{\mathrm{BB}'} = \frac{a}{b} \tag{1}$$

where a is half the aperture width of the PTC AA′ and b is half the aperture width of the receiver BB′.

The equation for the surface of the parabola in Cartesian co-ordinates is [11]:

$$y = \frac{1}{2f}x^2 \tag{2}$$

where the y axis is the axis of the PTC and f its focal length. The radius r from a point on the rim of the parabola to the focal point is given by the surface equation in polar co-ordinates:

$$r = 2f(1 + \cos\varphi)^{-1} \tag{3}$$

where φ is the rim angle.

The aperture width of the PTC is the projection of AA′ onto the plane normal to the incident rays (i.e. normal to the axis of the parabola) and is given by

$$a = r\sin\varphi = 2f\sin\varphi(1 + \cos\varphi)^{-1} \tag{4}$$

From Fig. 1,

$$b = a - 2f\cos\varphi(1 + \cos\varphi)^{-1}\tan(\varphi - \delta)$$

Substitution for a and b in Eq. (1) will give

$$Cr_{(\mathrm{PTC})} = \left(1 - \frac{\tan(\varphi - \delta)}{\tan\varphi}\right)^{-1} \tag{5}$$

Now, consider a compound parabolic concentrator (CPC) with entrance and exit apertures BB′ and CC′, respectively, separated so that an extreme ray BC′ (or B′C) makes the maximum collecting angle (θ) with the axis of the concentrator, as shown in Fig. 1. The concentration ratio (Cr_{CPC}) and the depth (D_{CPC}) of the CPC are given as [12]:

$$Cr_{\mathrm{CPC}} = \sin\theta^{-1} \tag{6}$$

$$D_{\mathrm{CPC}} = (b + c)\cot\theta \tag{7}$$

whereθ, the half acceptance angle is $\varphi - \delta$ Fig. 1. Therefore,

$$Cr_{\mathrm{CPC}} = (\sin(\varphi - \delta))^{-1} \tag{8}$$

The total concentration ratio of the combined concentrator (Cr_{TOT}) is the product of the concentration ratios of the primary and the secondary, thus

$$Cr_{\mathrm{TOT}} = \left[\sin(\varphi - \delta)\left(1 - \frac{\tan(\varphi - \delta)}{\tan \varphi}\right)\right]^{-1} \tag{9}$$

For maximum concentration, δ must be as small as possible compared with the rim angle. For a given parabolic reflector, δ is dependent on the width of the receiver. High concentration factors are achieved by using smaller receivers and, consequently, smaller tolerance angles, which require frequent tracking adjustment. However, the CPC becomes too deep at a high concentration ratio. In addition, its acceptance angle must match the incident angle of the source radiation (radiation reflected by the primary PTC). Careful selection of these two factors is essential to the design of an effective concentrator.

The aim here is to improve the performance of the system by appropriate selection of design parameters. One of these is the required concentration ratio. As shown in Eq. (9), the concentration ratio is a function of the rim angle and the permissible degree of tolerance to

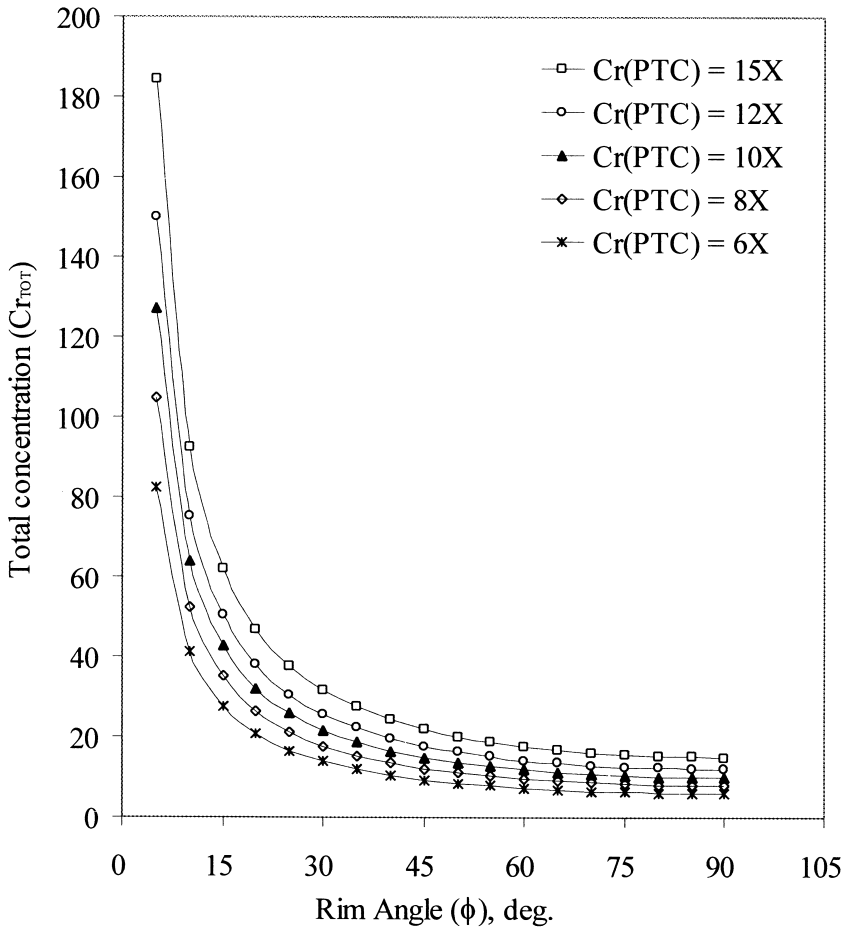

Fig. 2. Concentration ratio of the combined concentrator plotted against rim angle for various combinations of PTC and CPC.

misalign incoming sun rays. This, in turn, determines the precision of tracking adjustment which has to be provided for efficient concentration.

The variation of the concentration ratio with rim angle, for various combinations of PTC and CPC, is plotted in Fig. 2. These curves are obtained by solving Eq. (5) for δ for each combination and substituting its value in Eq. (9). Higher concentration ratios can be obtained by using a small rim angle but at the expense of other factors. One of these is the depth of the CPC, which needs to be limited. Another factor is the mechanical stability of the concentrating system. A small rim angle implies a large ratio of focal length to aperture width for the PTC. This means that the receiver will be far away from the centre of mass of the reflector. Such a system can be mechanically unstable, making rotation and tracking adjustment more difficult.

To improve the mechanical stability of the concentrating system, it is often appropriate to use a primary PTC with a large rim angle. For a given aperture, a large rim angle implies that the receiver is closer to the centre of mass of the collector. As a general rule, the optimum rim angle of parabolic trough concentrators for flat receivers is in the range 40–60° [13]. CPCs are suitable for acceptance half angles in the range up to about 40° [6]. This suggests that the

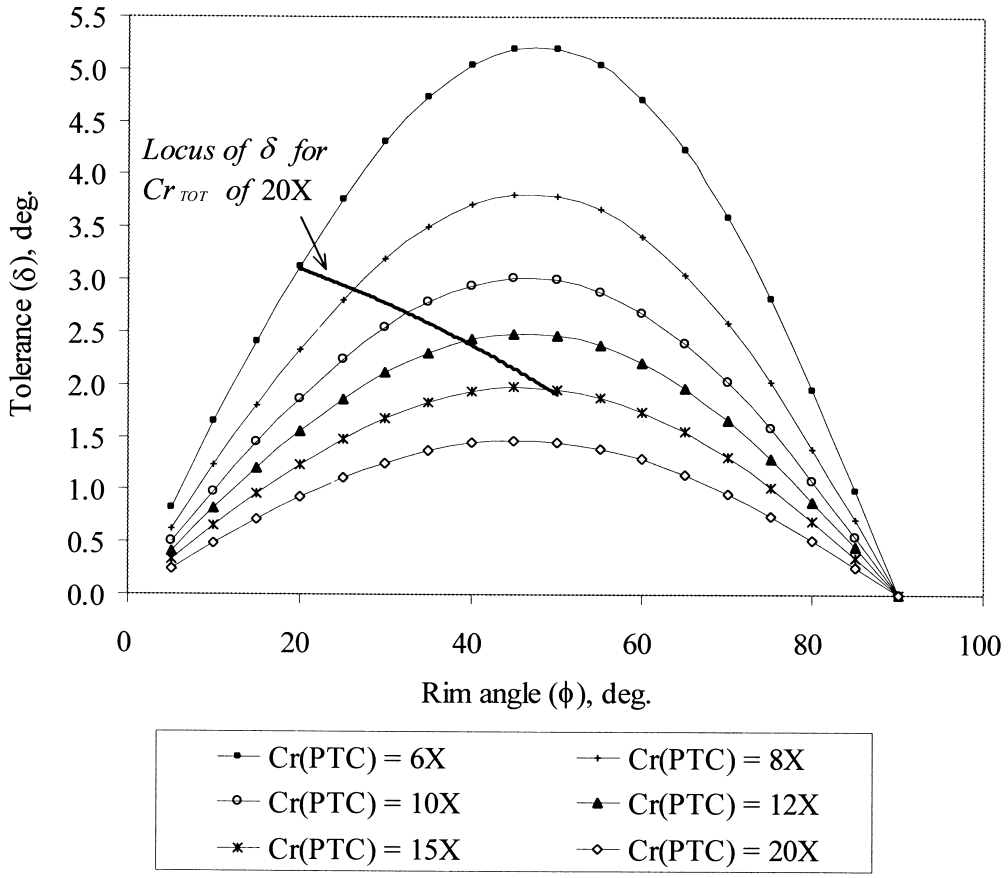

Fig. 3. Tolerance of incident rays as a function of PTC rim angle.

matching angle should be around 40°. The variation of the resulting tolerance with the rim angle, for various combinations of PTC and CPC, is plotted in Fig. 3. The locus of δ for different combinations of the required total concentration ratio of 20 is also shown. The maximum allowable tolerance that can be obtained by a single PTC concentrator with this concentration ratio is 1.47°. Introduction of a second stage will boost the tolerance angle, for instance, to 1.96°, 2.43°, 2.54°, 2.80° and 3.12° for combinations with a PTC of concentration factor 15, 12, 10, 8 and 6, respectively. In general, a larger tolerance can be obtained by combining a PTC with small concentration ratio and a CPC of a relatively large concentration ratio, while other factors, such as depth of the CPC, the matched CPC acceptance and PTC rim angles and the size of the receiver system, have to be taken into consideration.

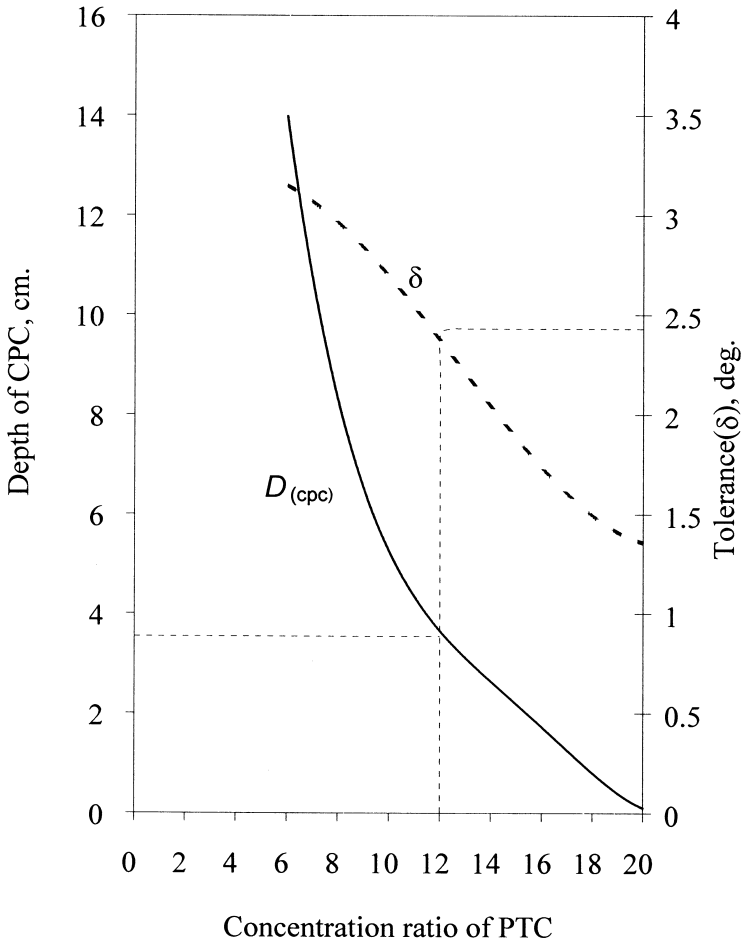

Fig. 4. Variation of the tolerance angle and the depth of the CPC with the concentration ratio of the PTC, showing design parameters.

2.2. Thermal and structural design considerations

An important aspect of the overall design is heat loss from the absorber. This can be reduced dramatically by enclosing the receiver system inside a glass envelope. This has the additional benefit of protecting the second stage reflector surface from the environment. With evacuated tubes, bare silver surface reflectors can be used. The size of the glass envelope is of concern, bearing in mind that a minimum air gap of about 6 mm may be necessary to avoid heat losses in cases when the glass tube is not adequately evacuated, in order to suppress convective heat loss [14]. Therefore the CPC depth should be such as to allow accommodation inside the glass tube with the minimum air gap. The depth of the CPC is reasonably small at large rim angles and increases with decreasing rim angle, to become excessive at low rim angles.

In order to determine which combination should be selected to give a total concentration ratio of 20, which has been shown to be appropriate for irradiating thermoelectric devices [15], the following steps have been followed. From Fig. 2, the rim angle at which each combination gives the required concentration ratio is determined. The corresponding degree of tolerance for each combination is determined using the locus of δ from Fig. 3. The final selection is based on the equivalent depth of the CPC that allows accommodation of the receiver system inside an appropriate glass tube. Fig. 4 shows the variation of the tolerance angle and the corresponding depth of the CPC across a range of primary concentrators for a total concentration of 20X.

The availability of the glass tube to accommodate the receiver system is an important practical consideration. Commercial light wall tubing glass that would suit solar energy

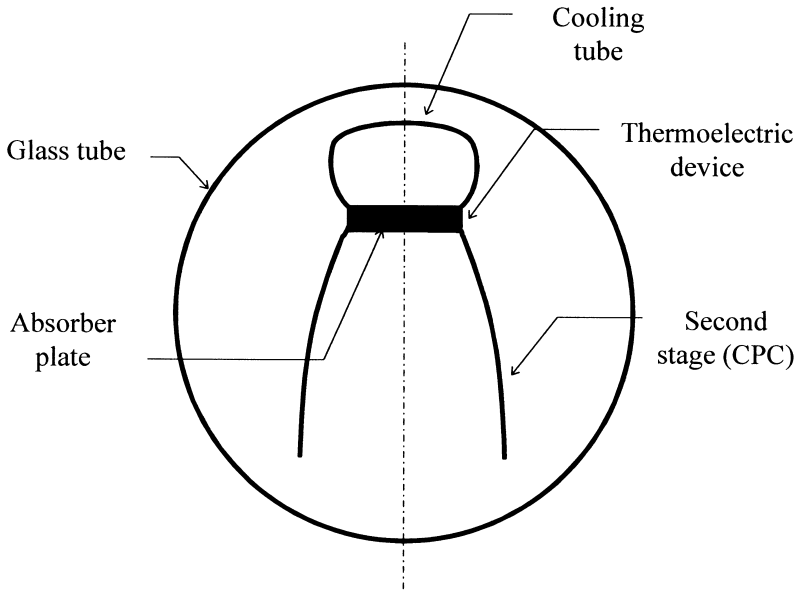

Fig. 5. Schematic diagram of the receiver system.

applications is available in sizes between 65 and 100 mm in diameter. For a total concentration ratio of 20, a combination of a PTC with a concentration of 12X and a CPC with a concentration of 1.67X is proposed. This allows a tolerance of about ± 2.45 at a rim angle of 40°, as shown in Fig. 4. Assuming an average daily change in the latitude of the sun at noon of about 0.2° per day, typical of equatorial regions, the tracking adjustment is needed only every 2 weeks at most. If one can afford a glass tube of larger diameter, a design with higher tolerance can be selected, though the corresponding rim angle will be smaller and, thus, the concentrator will be less stable mechanically.

The above approach to concentrator design is very versatile and can be applied for other concentration factors and geometries.

A cross section through the concentrator is shown in Fig. 5 with the secondary concentrator enclosed by a glass tube. The absorber plate of the thermoelectric device (hot junction) is placed at the focus of the CPC, and a tube for liquid coolant is fitted to the cold junction. A summary of the geometrical parameters of the combined concentrating system is given in Table 1.

3. Collector performance evaluation

An important aspect of the collector performance concerns the effect of the secondary PC and its role in improving the concentration efficiency and inhibiting convective heat loss from the absorber plate. The efficiency of a solar concentrator under steady state conditions is given by [16]:

$$\eta = \eta_o F_R - U_L F_R (G C_r)^{-1} (T_{in} - T_A) \tag{10}$$

where, F_R is the heat removal factor, U_L is the overall heat loss coefficient of the receiver system, C_r is the geometrical concentration ratio of the concentrating system, G is the total beam radiation measured in the plane of the PTC aperture, and T_{in} and T_A are the fluid inlet and ambient air temperatures, respectively. The term η_o is the optical efficiency of the concentrator and represents all the optical characteristics of the concentrating system, including the transmittance–absorptance product of the receiver system ($\tau\alpha$), the intercept factor (γ) and the effect of the multiple reflection process of the incoming rays. In principle, the value of the factor γ can be increased by using a wider receiver; an approach that led to consideration of the secondary concentrator.

Table 1
Geometrical design parameters for the solar concentrating system

PTC aperture width, (mm)	394	Rim angle of the PTC (deg)	40
PTC focal length (mm)	270	Concentration of the secondary	1.64
Concentration of the primary	12	CPC half acceptance angle (deg)	37.5
CPC aperture window (mm)	328	Diameter of the glass tube (mm)	70
Absorber plate width (mm)	20	Diameter of the cooling tube (mm)	22
Depth of the CPC (mm)	354	Total concentration ratio	19.7

The heat transfer processes associated with the receiver system are shown schematically in Fig. 6 and can be represented by a simplified electrical network, as shown in Fig. 7. The receiver system is divided into four main thermal parts, namely the absorber plate S, the CPC reflector R, the glass tube G and the cold plate C (which includes the cooling tube and the cold junction of the thermoelectric element).

The thermal resistance terms R_{SG}, R_{SR}, R_{RG}, R_{CG} and R_{GA} represent the thermal resistances to heat flow from the absorber surface to the glass tube, from the absorber to the CPC reflector, from the CPC reflector to the glass tube, from the cooling tube to the glass tube and from the glass tube to the ambient air, respectively

The value of the overall heat loss coefficient U_L in Eq. (10) depends on the magnitude of the convective, radiative and conductive heat losses. The conductive heat loss is limited, since there is no significant contact between the heated elements and the glass tube, except at the glass–

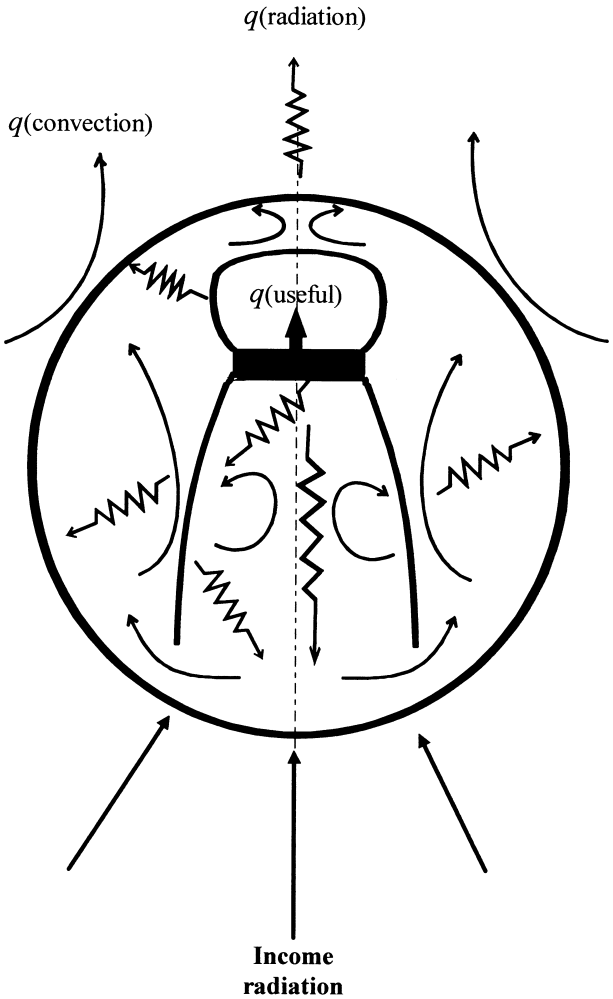

Fig. 6. Energy transfer processes associated with the receiver system.

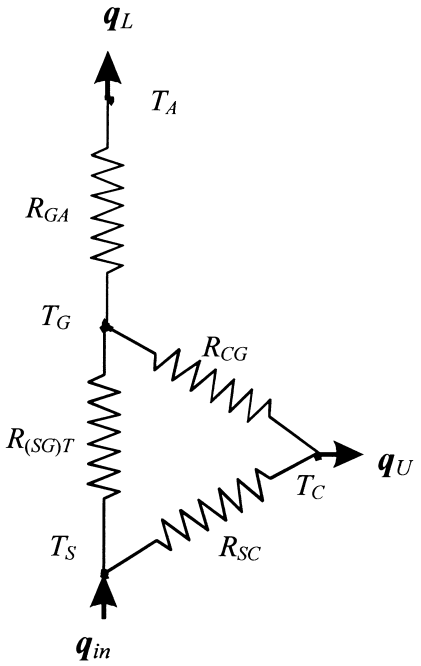

Fig. 7. Simplified electrical network analogue for heat flow in the receiver system.

metal bonding at the ends of the collector. Convective heat losses can, in principal, be greatly reduced by maintaining some level of vacuum inside the glass tube. A pressure level of 25–50 mm Hg adequately suppresses convection [17]. In this design, however, the proposed configuration is intended to reduce convective heat loss from the absorber plate, by trapping the hot air between the space confined by the absorber plate and the CPC reflector.

The overall heat loss coefficient can be estimated from the simplified thermal network as

$$U_{\mathrm{L}} = U_{\mathrm{GA}}\Big[1 + U_{\mathrm{GA}}U_{\mathrm{SC}}\big(U_{\mathrm{CG}}U_{\mathrm{SC}} + U_{\mathrm{CG}}U_{(\mathrm{SG})\mathrm{T}} + U_{\mathrm{SC}}U_{(\mathrm{SG})\mathrm{T}}\big)^{-1}\Big]^{-1} \tag{11}$$

where U_{GA}, U_{CG}, U_{SC} and $U_{(\mathrm{SG})\mathrm{T}}$ are the heat transfer coefficients between the glass tube and the surrounding environment, the cooling tube and the glass tube, the absorber plate and the cooling tube and the total heat transfer coefficient from the absorber surface to the glass tube (directly and via the CPC reflector), respectively.

Values of $\eta_{\mathrm{o}}F_{\mathrm{R}}$, and $U_{\mathrm{L}}F_{\mathrm{R}}$ in Eq. (10) can be calculated theoretically, or determined experimentally, following a standard procedure, from a plot of collector performance against $(T_{\mathrm{in}} - T_{\mathrm{A}})/G$.

As can be seen in Fig. 7, at the absorber surface with temperature T_{S}, the solar radiation $\boldsymbol{I}_{\mathrm{S}}$ is absorbed and distributed as thermal losses at temperature T_{A}, either directly through the glass tube at temperature T_{G} or via the CPC reflector at temperature T_{R}, or to the cooling tube at temperature T_{C}. The remainder of the absorbed energy is extracted as useful heat, expressed as:

$$Q_u = Q_{el} + \dot{m}C_p(T_o - T_{in}) \tag{12}$$

where $\dot{m}$ and C_p are the mass flow rate and the specific heat of the cooling fluid, T_{in} and T_o are the inlet and the outlet temperatures of the cooling fluid, respectively. Q_{el} is the electrical energy produced by the thermoelectric device and delivered to the load.

Finally, the overall solar collector efficiency is determined directly from

$$\eta = \frac{Q_u}{GA_{PTC}} \tag{13}$$

using experimentally determined values for Q_u, G and A_{PTC}.

3.1. Computational fluid dynamic analysis of trapped flows

FLUENT, the proprietary computational fluid dynamic code, has been used for modelling the convective motion of the air enclosed in the receiver. It is assumed that all the components of the receiver are thin and have negligible heat capacity. The temperature distribution along each surface is assumed to be uniform, and the receiver system is in thermal equilibrium. The temperature of the hot junction of the thermoelectric element is assumed to be the same as that of the absorber plate, and similarly, the temperature of the cold junction is assumed to be the same as that of the cooling tube. The overall solution was produced using a twin loop procedure: an inner loop computed using FLUENT (until solution convergence) and an outer loop for the external heat flow to determine iteratively the external heat transfer coefficient. The overall external heat transfer coefficient is initialised based on an estimate of the glass tube temperature and subsequently re-adjusted, following the FLUENT calculations, until convergence is achieved.

3.2. Experimental validation of the design

An experimental system was constructed consistent with the proposed design, Table 1. The PTC is comprised of an aluminium sheet formed onto a pre-shaped structural frame to give a

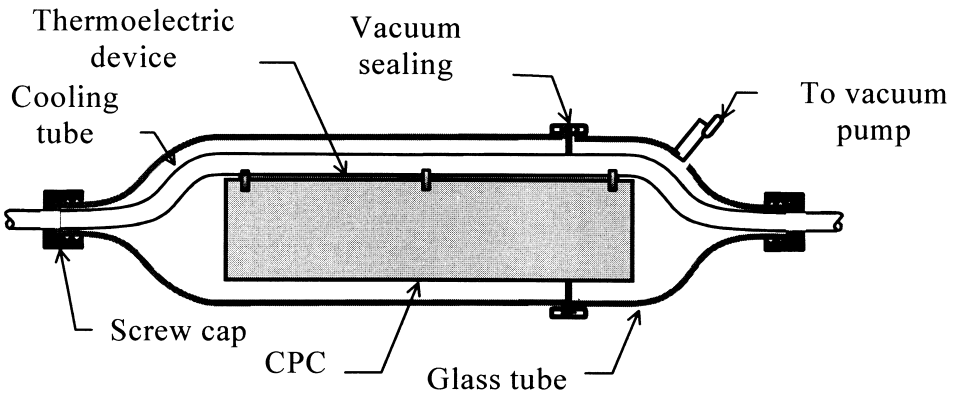

Fig. 8. Details of the experimental receiver system.

parabolic profile. The reflecting surface was provided by lining the aluminium sheet with an aluminised polymer film (mirror). The CPC was constructed of anodised aluminium sheet, cut to give parabolic segments. The CPC was attached to the cooling tube, which is flattened on one side to allow good thermal contact with the thermoelectric device. Several Peltier thermoelectric cooling devices were placed on the flat surface of the cooling tube using an acrylic adhesive heat sink bonder. In this experiment, these devices are not intended to function as power generators, but to provide the correct thermal properties between the absorber plate and the cooling tube. The absorber surface was formed using black paint on the receiver surface of the thermoelectric device. It is known that a thermoelectric efficiency of only a few percent can be expected, so that little influence on the measured temperature results from the lack of electrical connection of the devices. The glass envelope was prepared from Pyrex glass using flange joints and vacuum sealing rings arranged as shown in Fig. 8. The two ends of the glass tube were drawn down to fit the cooling tube and sealed using a sleeve gasket and hollow screw caps made of heat resistant phenolic plastic. The experimental investigation included the measurement of the input radiation and the heat extracted from the cold junction of the thermoelectric element, as well as the temperature distribution inside the receiver system. The tests were designed to assess the effect of three main parameters: namely the tracking misalignment, the collector inclination and the pressure level inside the glass tube. The experiment was conducted indoors, using a solar simulator based on two 1000 W Compact Source Iodide (CSI) lamps.

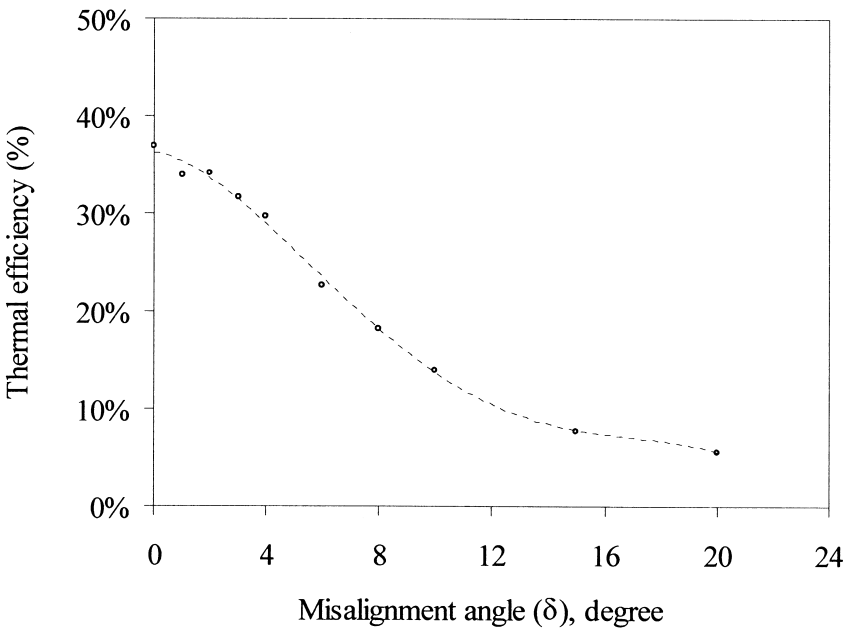

Fig. 9. Variation of the thermal conversion efficiency with collector misalignment angle at atmospheric pressure.

3.3. Discussion of system performance

The variation of the thermal conversion efficiency with tracking misalignment and collector tilt angle is shown in Figs. 9 and 10, respectively, with the tube enclosure at atmospheric pressure. As can be seen, the efficiency is very sensitive to the collector tracking misalignment angle, particularly for angles greater than about 4°.

The effect of the tilt angle on the performance of the concentrating system is minimal for angles less than 30° as shown in Fig. 10. As the tilt angle increases, the region confined by the absorber plate, the aperture window of the glass tube and the CPC reflector forms a deep horizontal cavity, resulting in a tendency to unicellular flow within this region. This can be seen from the plots of the stream functions and the isotherms obtained from the numerical solution, shown in Figs. 11 and 12, respectively. As can be seen, the flow field and the isotherms are determined by the tilt angle of the collector. The main thermal regions that can be observed are the region confined by the CPC reflector, aperture window and the absorber plate, the two side regions between the glass tube and the CPC reflector and, finally, the top region between the cooling tube and the glass tube.

The first is the region where heat may be transferred from the absorber plate to the glass tube directly or via the CPC. For a vertical orientation, a large central stable thermal plume of low multi-cellular flow and low temperature gradients dominates this region. Both the thermal gradients and the flow in this region start to increase and distort with the tilt angle. The multi-cellular pattern decreases with the tilt angle, forming nearly complete circulation at about 40° of tilt.

The second and the third regions form a unicellular flow with high upward and downward flow velocity for a vertically aligned receiver. These two regions are dominated by high temperature gradients near the CPC reflector and the glass tube, which are determined by the thermal properties of the CPC material and the external heat transfer coefficient. The centres

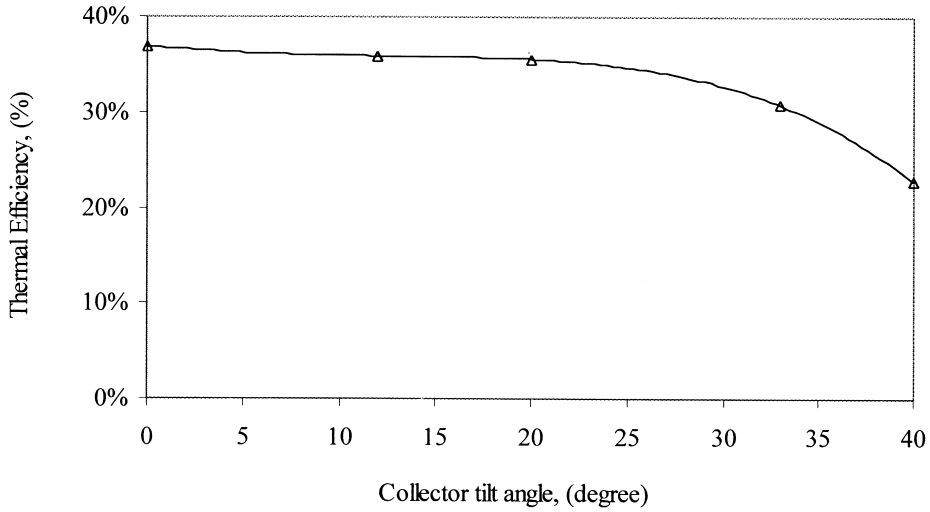

Fig. 10. Variation of the thermal conversion efficiency with tilt angle at atmospheric pressure.

of these regions exhibit somewhat stagnant flow, which is not strongly dependent on the tilt angle. At the vertical position or at small tilt angles, heat transfer to these regions is expected to be mainly by conduction through the CPC reflector, rather than through the gap at the bottom of the CPC reflector. As the tilt angle increases, heat flow through the right hand gap

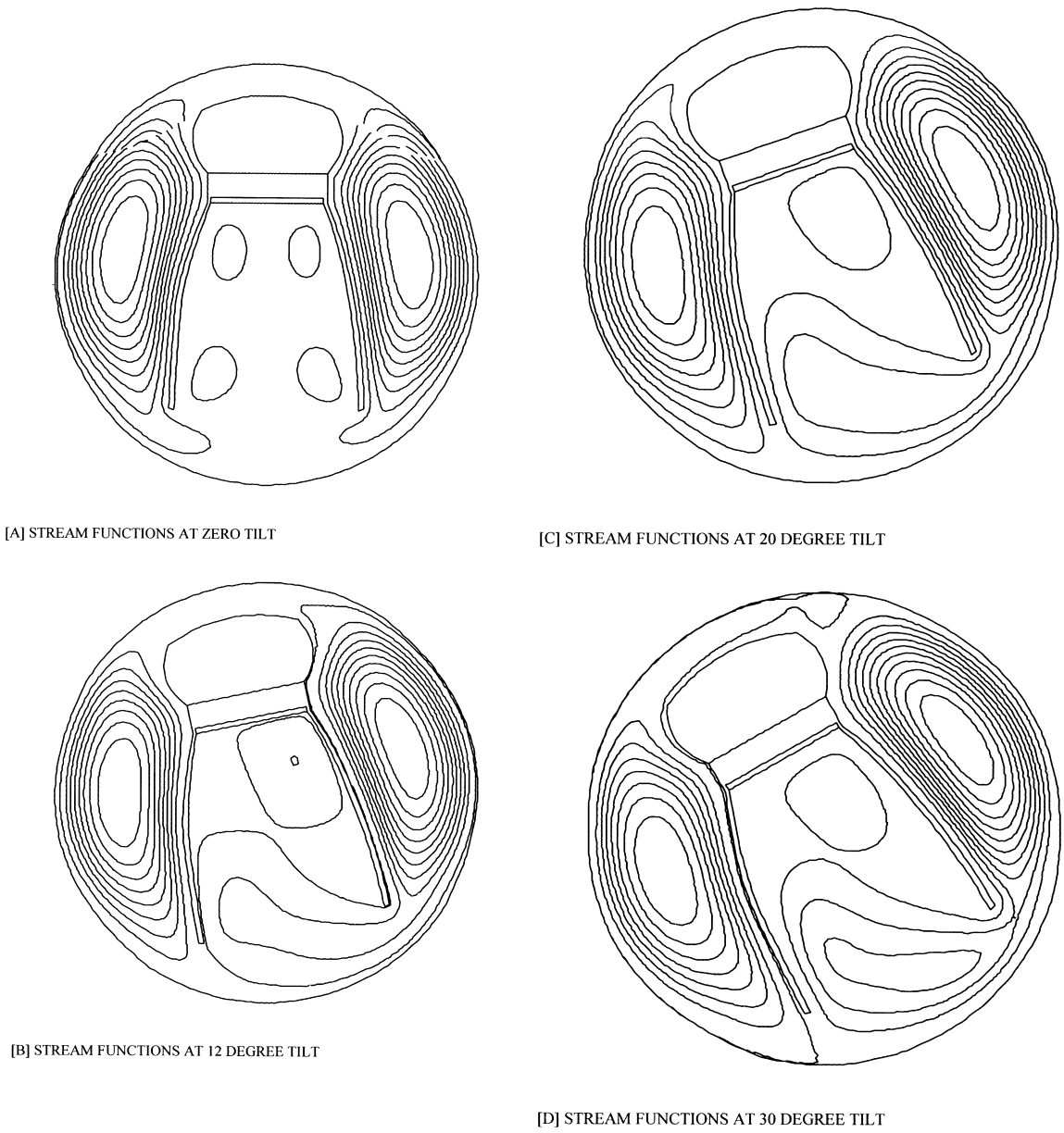

Fig. 11. Contours of stream functions of the flow field in the solar collector receiver: (A) vertically aligned receiver, (B) 12° tilt receiver, (C) 20° tilt receiver, (D) 30° tilt receiver, (E) 40° tilt receiver.

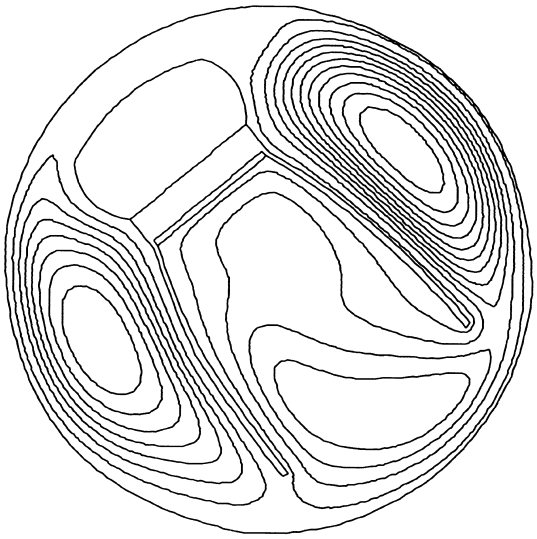

[E] STREAM FUNCTIONS AT 40 DEGREE TILT

Fig. 11. (*continued*)

starts to increase, as shown by the stream functions in Fig. 11. Generally, this element of the heat flow is small, even at high angles, due to the particular circulating flow pattern which occurs. These results indicate the importance of using material with low thermal conductivity for the CPC reflector and minimising the gap between the glass tube and the lower ends of the CPC reflector, which is usually limited because of practical concerns regarding the size of the glass tube.

The fourth region above the cooling tube also exhibits very low flow velocity and high temperature gradients, indicating that the heat transfer is dominated by conduction. This is because the gap between the cooling tube and the glass is too small for convection currents to become established.

Fig. 13 compares the calculated and the measured instantaneous performance of the concentrating system. The results predicted under vacuum conditions and those measured at 50 mbar are generally in reasonable agreement, particularly at low operating temperatures. As the operating temperature increases, the analytical model overestimates the performance, mainly because of the assumptions regarding the temperature independent surface radiation properties. It seems that the surface radiation properties of some components change significantly with the temperature, resulting in higher than expected radiative heat losses at high operational temperatures. In general, irrespective of the operating pressure, the efficiency curves are generally flat, indicating that the performance remains high even at elevated temperatures.

The key performance parameters describing the collector system ($F_R\eta_o$ and $F_R U_L$) were obtained from the data presented in Fig. 13 using least squares fitting. The calculated value of $F_R\eta_o$ under vacuum conditions was 0.40, while the measured values at 50 mbar and at

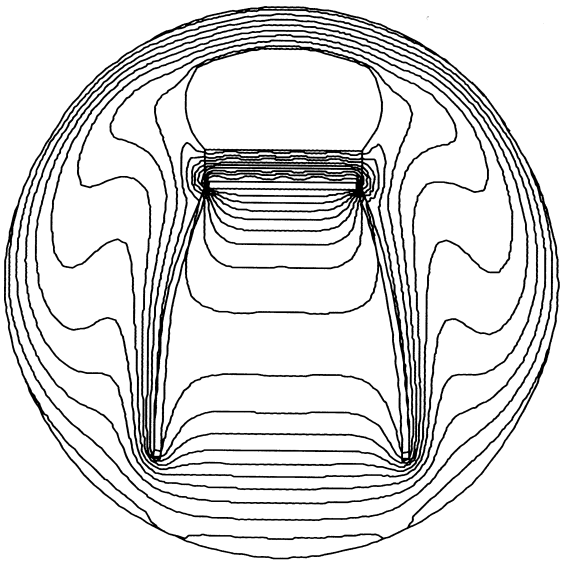

[A] ISOTHERMS AT ZERO TILT

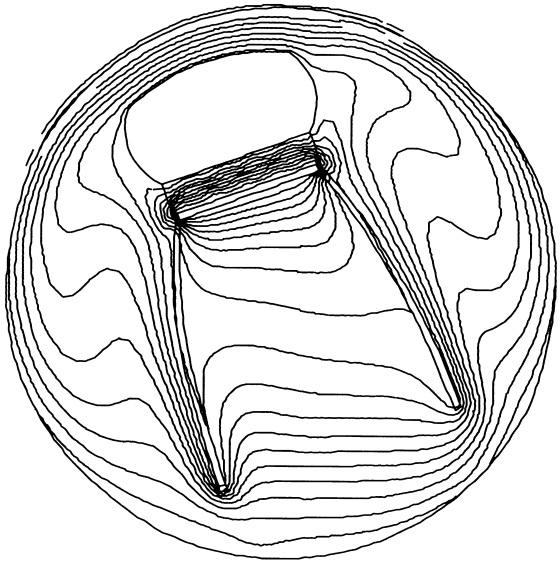

[C] ISOTHERMS AT 20 DEGREE TILT

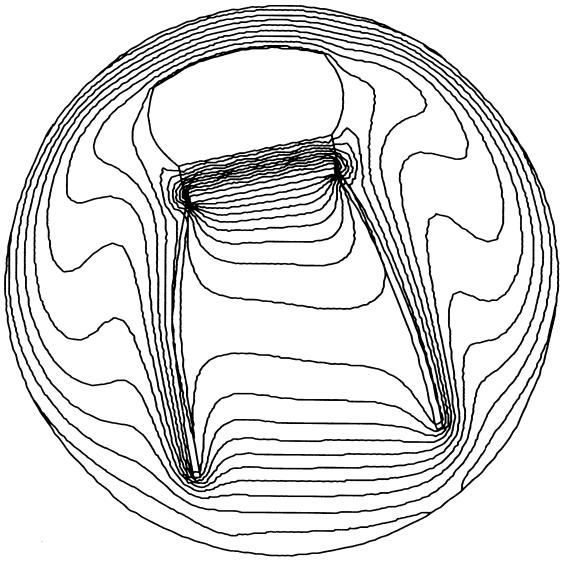

[B] ISOTHERMS AT 12 DEGREE TILT

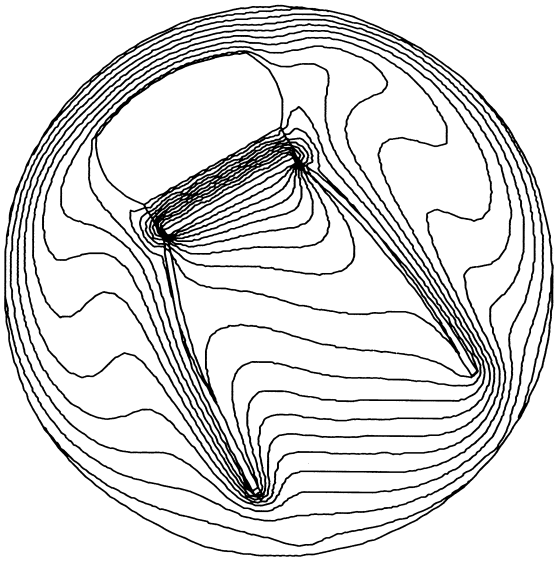

[D] ISOTHERMS AT 30 DEGREE TILT

Fig. 12. Contours of the isotherms in the solar collector receiver: (A) vertically aligned receiver, (B) 12° tilt receiver, (C) 20° tilt receiver, (D) 30° tilt receiver, (E) 40° tilt receiver.

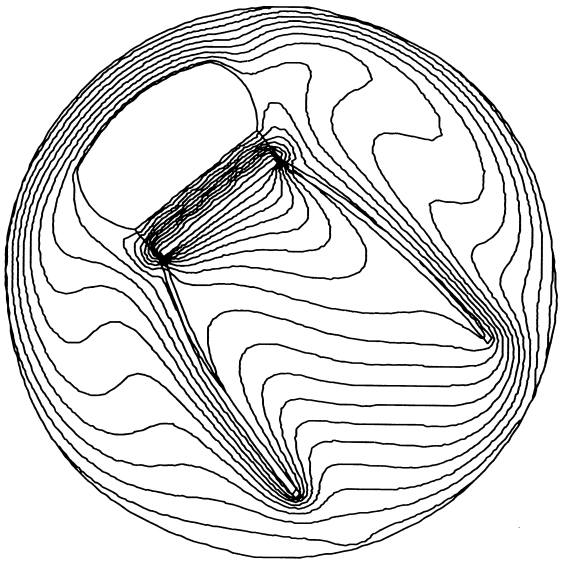

[E] ISOTHERMS AT 40 DEGREE TILT

Fig. 12. (*continued*)

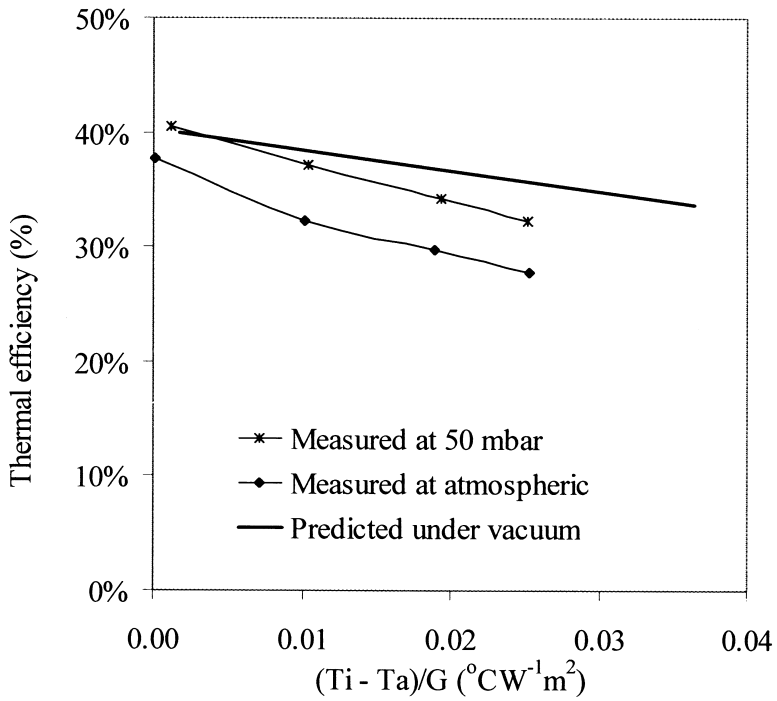

Fig. 13. Instantaneous thermal performance of a vertically aligned solar concentrator.

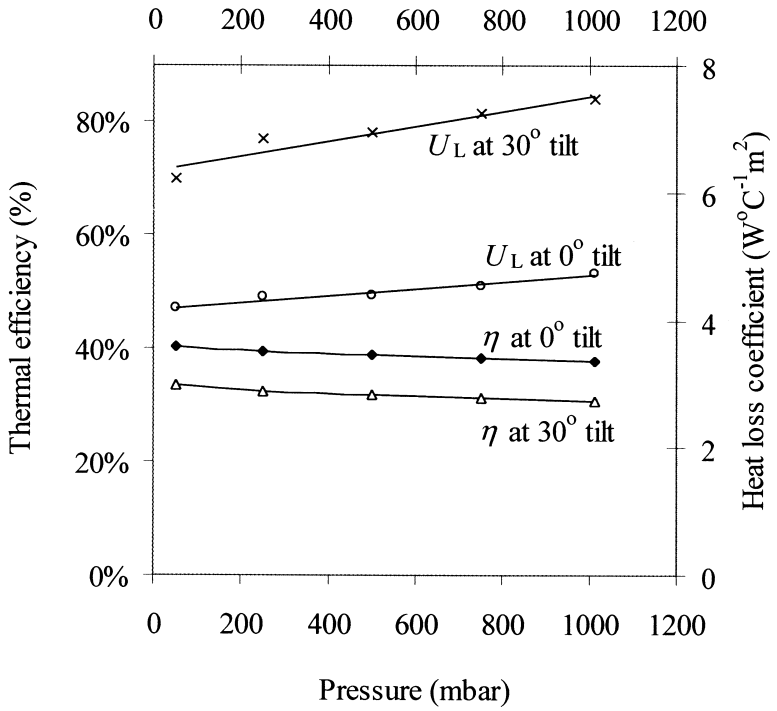

Fig. 14. Variation of the thermal conversion efficiency and the overall heat loss coefficient with pressure level inside glass tube.

atmospheric pressure were 0.41 and 0.38, respectively. The corresponding values of $F_R U_L$ under vacuum, 50 mbar and atmospheric pressure were 1.8, 3.5 and 3.9, respectively.

The variation of the thermal conversion efficiency and the heat loss coefficient with pressure, for vertically aligned and 30° tilted receivers, is shown in Fig. 14. The effect of the tilt angle is appreciable, but the effect of the pressure level inside the glass tube is insignificant in both cases. This indicates that thermal radiation rather than convection dominates the heat losses. The overall heat loss coefficient varied slightly with both the pressure level and the tilt angle. Reduction of the pressure from atmospheric to 50 mbar is accompanied by an 11% reduction in the value of U_L at zero tilt angle and by a 16% reduction at 30° tilt.

4. Conclusions

A design methodology has been developed for a two stage concentrator, tolerant of tracking misalignment, and this has been successfully applied to the design of a small combined heat and thermoelectric power generation unit. The resulting system has been assessed using computational fluid dynamic modelling. A laboratory scale system was tested using a solar simulator. The design has been demonstrated to provide efficient concentration of the incident solar radiation without the need for frequent tracking adjustment, indeed, results have shown

that the system can tolerate misalignment angles as high as 4° without a significant drop in the thermal performance.

References

[1] Gao M, Rowe DM. Optimization of thermoelectric module geometry for "waste" heat electric power generation. J. of Power Source 1992;38:253–9.
[2] Matsuura K, Rowe DM, Tsuyoshi AS, Min G. Large-scale thermoelectric generation of low-grade heat. In: Rowe DM, editor. Proc. 10th International Thermoelectric Conference. Cardiff, UK: University of Wales, 1991.
[3] Omer SA. Solar thermoelectric system for small-scale power generation. PhD Thesis, Loughborough University, UK, 1997.
[4] Rabl A. Optics and thermal properties of compound parabolic concentrators. Solar Energy 1976;18:497–511.
[5] Winston R. Principle of solar concentrators of a novel design. Solar Energy 1974;16:89–95.
[6] Rabl A. Comparison of solar concentrators. Solar Energy 1976;18:93–111.
[7] Collares-Pereira M, et al. High concentration two-stage optics for parabolic trough solar collectors with tubular absorber and large rim angle. Solar Energy 1991;47(6):457–66.
[8] Brunotte M, Goetzberger A, Blieske U. Two stage concentrator permitting concentration factors up to 300X with one axis tracking, Solar Energy 1996;50(3):285–300.
[9] Mills DR. Two stage tilting solar concentrators. Solar Energy 1980;25:505–9.
[10] Mills DR. Two stage solar collectors approaching maximal concentration. Solar Energy 1980;54(1):41–7.
[11] Pettofrezzo AJ, Lacatena MM. Analytical geometry with vectors. Scott: Foresman Press, 1970.
[12] Welford WT, Winston R. The optics of non-imaging concentrators: light and solar energy. London: Academic Press, 1978.
[13] Rabl A, Bendt P, Goal HW. Optimisation of parabolic trough solar collectors. Solar Energy 1982;29(5):407–17.
[14] Ratzel AC, et al. Techniques for reducing thermal conduction and natural convection heat losses in annular receiver geometry. Journal of Heat Transfer 1979;101:108–13.
[15] Omer SA, Infield DG. Design optimisation of thermoelectric devices for solar power generation. Solar Energy Materials and Solar Cells 1998;53(1–2):67–82.
[16] Duffie JA. Solar energy thermal processing. New York: Wiley, 1974.
[17] Duffie JA, Beckman WA. Solar engineering of thermal processes, 2nd ed. New York: Wiley, 1991.